



**HAL**  
open science

## Piezoelectric-actuated, piezoresistive-sensed circular micromembranes for label-free biosensing applications

Thomas Alava, Fabrice Mathieu, P. Rameil, Y. Morel, Caroline Soyer, Denis Remiens, Liviu Nicu

► **To cite this version:**

Thomas Alava, Fabrice Mathieu, P. Rameil, Y. Morel, Caroline Soyer, et al.. Piezoelectric-actuated, piezoresistive-sensed circular micromembranes for label-free biosensing applications. *Applied Physics Letters*, 2010, 97, pp.093703-1-3. 10.1063/1.3486112 . hal-00567894

**HAL Id: hal-00567894**

**<https://hal.science/hal-00567894>**

Submitted on 30 May 2022

**HAL** is a multi-disciplinary open access archive for the deposit and dissemination of scientific research documents, whether they are published or not. The documents may come from teaching and research institutions in France or abroad, or from public or private research centers.

L'archive ouverte pluridisciplinaire **HAL**, est destinée au dépôt et à la diffusion de documents scientifiques de niveau recherche, publiés ou non, émanant des établissements d'enseignement et de recherche français ou étrangers, des laboratoires publics ou privés.

# Piezoelectric-actuated, piezoresistive-sensed circular micromembranes for label-free biosensing applications

Cite as: Appl. Phys. Lett. **97**, 093703 (2010); <https://doi.org/10.1063/1.3486112>

Submitted: 06 May 2010 • Accepted: 13 July 2010 • Published Online: 02 September 2010

T. Alava, F. Mathieu, P. Rameil, et al.



View Online



Export Citation

## ARTICLES YOU MAY BE INTERESTED IN

[Parallel atomic force microscopy using cantilevers with integrated piezoresistive sensors and integrated piezoelectric actuators](#)

Applied Physics Letters **67**, 3918 (1995); <https://doi.org/10.1063/1.115317>

[Mode dependent fluid damping in pre-stressed micro-diaphragm resonators](#)

Journal of Applied Physics **124**, 235305 (2018); <https://doi.org/10.1063/1.5075545>

[A review on nanomechanical resonators and their applications in sensors and molecular transportation](#)

Applied Physics Reviews **2**, 021301 (2015); <https://doi.org/10.1063/1.4916728>

Lock-in Amplifiers  
up to 600 MHz



Zurich  
Instruments



## Piezoelectric-actuated, piezoresistive-sensed circular micromembranes for label-free biosensing applications

T. Alava,<sup>1</sup> F. Mathieu,<sup>1</sup> P. Rameil,<sup>2</sup> Y. Morel,<sup>2</sup> C. Soyer,<sup>3</sup> D. Remiens,<sup>3</sup> and L. Nicu<sup>1,a)</sup>

<sup>1</sup>LAAS, CNRS, 7, Avenue du Colonel Roche, F-31077 Toulouse, France

<sup>2</sup>DGA Maitrise MNRBC, DGA/DT/CEB, 5 Rue Lavoisier, 91710 Vert le Petit, France

<sup>3</sup>University of Lille Nord de France, F-59000 Lille, France

(Received 6 May 2010; accepted 13 July 2010; published online 2 September 2010)

In this paper, we report on the fabrication and characterization of the dynamic behavior of circular micromembranes integrating a piezoelectric thin film for actuation and a boron-doped silicon piezoresistor for sensing purposes. Resonant frequencies corresponding to high-order modes of vibration are measured, respectively, in air and deionized water. The measurements are compared with theoretical values calculated using the extended Lamb's model [H. Lamb, Proc. R. Soc. London **98**, 205 (1920)] adapted to the microscale. Moreover, label-free detection of *Bacillus atrophaeus* (or *B. atrophaeus*) with a concentration of  $10^8$  spores/mL is repeatedly performed in real-time which assesses the biosensing potential of microscale circular membranes bearing actuation and sensing elements. © 2010 American Institute of Physics. [doi:10.1063/1.3486112]

Despite recent technological breakthroughs promoting all-polymer<sup>1</sup> or even paper<sup>2</sup> biosensors, silicon-based devices still represent the golden path toward label-free biosensing platforms satisfying high performance standards. It is now expected even to integrate such miniaturized biosensors onto mobile phones for real-time basic biomarkers (glucose, urea, etc.) monitoring.<sup>3</sup> In the silicon-based sensors field, resonant microelectromechanical systems (or MEMS)-based physical sensors, inspired by the Sauerbrey's seminal description of the quartz microbalance principle,<sup>4</sup> are among the best candidates to biosensing. The operation principle may be resumed as follows: as the squared mechanical resonant frequency is in inverse proportion with the sensor's mass, any added mass to its surface would be instantly translated into a resonant frequency shift. The lightest sensor would be thus the most sensitive. This involves ultimate downsizing while integrating onto the sensor's structure actuation and detection functionalities. So far, several actuating/sensing schemes have been considered for biosensing purposes but they rapidly revealed technological limitations: magnetomotive (integration-limited as it requires an external magnet<sup>5</sup>), piezoresistive (highly sensitive but ineffective as actuator<sup>6</sup>), piezoelectric (ineffective for sensing applications as it requires high-gain/wide band charge-amplifying solutions<sup>7</sup>). In order to choose the best solution for the required function, we made the choice of coupling the piezoelectric actuation to piezoresistive sensing onto the same micromechanical structure. Though the piezoelectric actuation/piezoresistive sensing is appealing in terms of potential performances, only few attempts of such a physical cointegration have been reported in the past.<sup>8,9</sup> The mechanical structure geometry is another major issue when dealing with silicon-based bioMEMS. The cantilever structure has a proven track record in the biosensing area.<sup>10</sup> Nevertheless, key limitations dramatically shrink the use of cantilevers as effective label-free biosensors: they are brittle and, they exhibit low quality factors. Since a couple of years, attempts have been made to propose alternative solutions to the well-established cantilever design like

disk-like shaped structures,<sup>11</sup> tuning forks,<sup>12</sup> film bulk acoustic resonators,<sup>13,14</sup> or membranes.<sup>15–19</sup>

In this paper, we report on the fabrication and characterization of the dynamic behavior of circular micromembranes integrating a piezoelectric thin film for actuation and a boron-doped silicon piezoresistor for sensing purposes. Resonant frequencies measured in deionized water are compared with theoretical values calculated using the extended Lamb's model<sup>20</sup> adapted to the microscale. Label-free detection of *B. atrophaeus* is performed in real-time using specific antibodies<sup>21</sup> grafted onto the circular micromembrane's surface prior to the biorecognition experiments.

Chips ( $7.2 \times 6.4$  mm<sup>2</sup>) of five micromembranes have been realized by standard microfabrication techniques from 4 in. (100) N-type silicon-on insulator (SOI) wafers (5  $\mu$ m device layer, 1  $\mu$ m buried oxide, 525  $\mu$ m handle). Each membrane (external radius hereafter labeled by  $R_M$ , values given in Ref. 24) is actuated by a 1  $\mu$ m thick rf-magnetron 54/46 PbZr<sub>x</sub>Ti<sub>1-x</sub>O<sub>3</sub> (PZT) patch of radius hereafter identified by  $R_{PZT}$  patterned on top of the membrane. According to previous works<sup>22</sup> the ratio  $R_{PZT}/R_M$  has been chosen equal to 0.5 to have the best actuation efficiency. The detection of the membrane's vibration is realized by a piezoresistor (20° angular aperture, 200 nm thick and 10  $\mu$ m width) located at its very periphery. The detailed process fabrication process has been described elsewhere.<sup>23</sup> Figure 1 shows the scanning electron microscope picture of a circular micromembrane.

After separating the individual dies, each one is glued onto a dedicated printed card board (PCB) and contact pads gold-wired to the PCB pins. The bonding wires are protected by a H20E-2 embedding gel (Polytech, France). The membranes' top electrodes are gathered to a common ground electrical plan while the bottom electrodes are individually biased.

First, resonant frequency measurements have been performed in multiplexed mode, in air and in deionized water. Frequency scans on five different channels,<sup>24</sup> each corresponding to one specific membrane, were possible due to a dedicated analog electronics specifically designed and assembled<sup>23</sup> for this application. See Ref. 24 for a summary

<sup>a)</sup>Electronic mail: nicu@laas.fr.

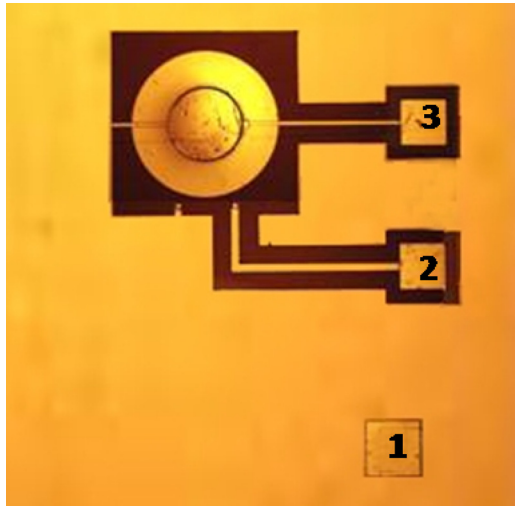


FIG. 1. (Color online) Optical microscope photo of a fabricated  $440\ \mu\text{m}$  radius micromembrane. Electrical contact pads correspond to (1) the common ground, (2) the piezoresistor's polarization current input, and (3) the piezoelectric module's bottom electrode. The common ground stands for the piezoelectric module's top electrode as well as the piezoresistor's polarization current output.

of the measured resonant frequencies in air and liquid (as well as the corresponding quality factors) for the first three modes of vibration presenting a nodal circle, i.e., modes  $(0,i)$  with  $i=0,2$ . We focused on these modes as their shape present no risk of undetectable resonant frequency with respect to the piezoresistor's position (compared to the case of a nodal diameter mode which symmetry could cancel the piezoresistor's variation due to opposite sign stresses). We used the extended Lamb's model<sup>20</sup> to analytically determine the theoretical values (see Ref. 24) of the membranes' resonant frequencies in liquid. The model is based on the seminal works of Lamb who proposed in 1920 a theoretical model<sup>25</sup> that allows estimating the shift in the resonant frequency

from vacuum to water of a thin circular plate filling an aperture in a plane (and rigid) wall which is in contact on one side with an unlimited mass of water. The model proposed in Ref. 20 broadens the potential of the initial Lamb's model [originally restricted to the  $(0,0)$  resonant mode] in that sense that theoretical resonant frequencies in liquid may be estimated for higher-order modes. Starting from the measured resonant frequencies in air as well as taking into account the multilayered structure of the membranes and the corresponding added virtual mass incremental factor of each considered vibrating mode,<sup>20</sup> made it possible the calculation of the resonant frequencies in liquid. It should be noted that the higher the mode's order is, the better the agreement between theory and experience is. The main reason might be the fact the membranes' mode shapes in liquid are less affected by the liquid as the mode's order is increasing.<sup>20</sup> The extended Lamb's model along with the measured quality factors allowed estimating the micromembranes' mass sensitivities and minimum detectable masses in liquid. In the case of the largest membrane (radius of  $440\ \mu\text{m}$ ) vibrating on its  $(0,1)$  mode, for instance, the mass sensitivity<sup>7</sup> and mass resolution values are respectively equal to  $0.27\ \text{pg/Hz}$  and  $70\ \text{pg}$  which are about one order of magnitude better when compared to the state-of-the-art liquid mass microsensors.<sup>26</sup>

To demonstrate the biosensing potential of the self-actuated/self-sensed membranes, we chose an immunosensing scheme based on the detection of *B. atrophaeus* spores which are commonly used as biological warfare agent (BWA) surrogates. Antibodies against *B. atrophaeus* were produced in rabbits, purified and quantified. Solutions containing  $50\ \mu\text{g/mL}$  antibodies were prepared by dilution in phosphate buffer saline (PBS,  $0.05\ \text{M}$ ,  $\text{pH}\ 7.4$ ). Antibodies were covalently immobilized on gold-coated micromembranes via a self-assembled monolayer of thiols. The micromembranes' chip was immersed overnight, in the dark, in a solution of 11-mercaptoundecanoic acid ( $5\ \text{mM}$  MUA in

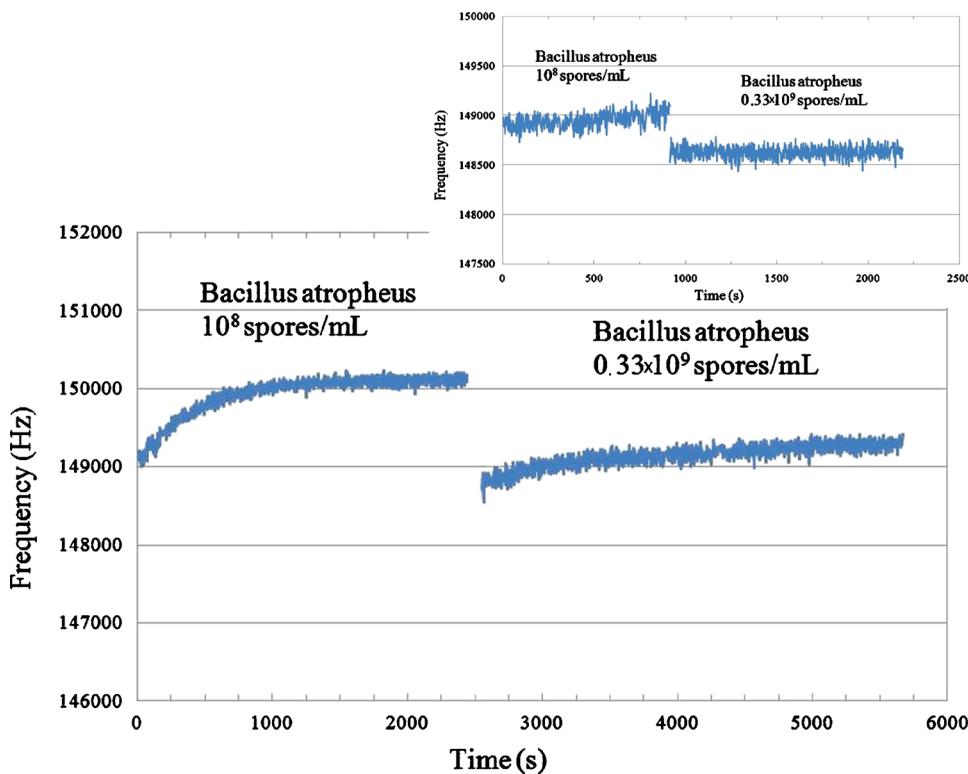


FIG. 2. (Color online) Real-time  $(0,1)$ -mode resonant frequency shifts of a  $440\ \mu\text{m}$  radius membrane when exposed to solutions of *B. Atrophaeus* (at respectively,  $0.33 \times 10^9$  spores/mL and  $10^8$  spores/mL). The inset shows the sensor's response after surface regeneration and repetition of the same *B. Atrophaeus* biological recognition cycle. The counterintuitive increase in the resonant frequency during the first seconds of mass uptake by the sensor is due to the thermal equilibrium reached by the antigen drop which initial temperature ( $25\ ^\circ\text{C}$ ) is lower than the chip's one ( $34\ ^\circ\text{C}$ ) heated by the associated electronics placed underneath the sensor.

absolute ethanol). It was then washed in absolute ethanol, next in water and dried under a stream of nitrogen. To activate carboxyl groups of surface-coated MUA, a 300  $\mu\text{L}$  solution containing 50 mM N-hydroxy-succinimide (NHS) and 200 mM N-Ethyl-N'-(3-dimethylaminopropyl)carbodiimide in PBS buffer was deposited onto the sensors' surface for 20 min. Immediately afterwards, pure PBS was flushed over the chip for 5 min. Anti-*B. atrophaeus* antibodies (30  $\mu\text{L}$  solution, concentration of 100  $\mu\text{g}/\text{mL}$ ) diluted in PBS 1 $\times$  were then deposited on the membranes' surface and left until surface saturation was reached (60 min). PBS 1 $\times$  was then flushed over the chip to wash out any unbound antibody. At the end, unreacted binding sites were saturated with ethanolamine (1 M, pH 8.5, 30 min). Two solutions containing decreasing amounts of *B. atrophaeus* (at respectively,  $0.33 \times 10^9$  spores/mL and  $10^8$  spores/mL) were prepared by dilution in PBS 1 $\times$  from mother solution containing  $1.4 \times 10^9$  spores/mL. The less concentrated *B. atrophaeus* solution (volume of 300  $\mu\text{L}$ ) was first deposited and left to incubate during 50 min, followed by a PBS 1 $\times$  rinsing step and the deposition of the most concentrated solution (in the same volume and same time of incubation conditions as the previous one). The corresponding real-time (0,1)-mode resonant frequency shifts in case of a 440  $\mu\text{m}$  radius membrane are shown in Fig. 2. The deposition of a 150  $\mu\text{L}$  drop of 130 mM NaOH allowed the cleavage of the antibodies-antigens bonds and the subsequent regeneration of the sensor's surface. We repeated the *B. atrophaeus* biological recognition cycle as previously described (see the inset on Fig. 2). Despite the counterintuitive increase in the resonant frequency value during mass uptake by the sensor before saturation in the very first seconds of the reaction, the difference between the stabilized resonant frequencies levels ( $\sim 600$  Hz) is reproducible after regeneration and corresponds to an added mass of 162 pg. The increase in the resonant frequency is due to the thermal equilibrium reached by the antigen drop which initial temperature (25  $^\circ\text{C}$ ) is lower than the chip's one (34  $^\circ\text{C}$ ) heated by the associated electronics placed underneath the sensor.

In summary, we were able to demonstrate the effective cointegration of piezoelectric actuation and piezoresistive sensing schemes onto individual microscale circular membranes. Multiplexed resonant frequency measurements in air and deionized water were performed and allowed estimating the mass-sensing capabilities of the micromembranes. Mainly, the mass sensitivity (0.27 pg/Hz) and mass resolution (70 pg) could be calculated by making use of the analytical extend Lamb's model which was proven to be well adapted to rapid prototyping of this generation of biosensors.

Furthermore, the real-time label-free biosensing capabilities of the circular micromembranes were demonstrated by performing a complete biological immunosensing protocol on chip for the detection of *B. atrophaeus* used as BWA surrogate.

T.A., F.M., C.S., D.R., and L.N. gratefully acknowledge the French General Delegation of Armament for the financial support of this project under REI/MRIS Grant No. 06.34.025 as well as the support of T.A.'s PhD thesis work.

- <sup>1</sup>C. Y. Li, P. M. Wu, W. Jung, C. H. Ahn, L. A. Shutter, and R. K. Narayan, *Lab Chip* **9**, 1988 (2009).
- <sup>2</sup>A. W. Martinez, S. T. Phillips, M. J. Butte, and G. M. Whitesides, *Angew. Chem., Int. Ed.* **46**, 1318 (2007).
- <sup>3</sup>J. M. Ruano-López, M. Agirregabiria, G. Olabarria, D. Verdoy, D. D. Bang, M. Q. Bu, A. Wolff, A. Voigt, J. A. Dziuban, R. Walczak, and J. Berganzo, *Lab Chip* **9**, 1495 (2009).
- <sup>4</sup>G. Z. Sauerbrey, *Z. Phys.* **155**, 206 (1959).
- <sup>5</sup>C. Vančura, Y. Li, J. Lichtenberg, K. U. Kirstein, A. Hierlemann, and F. Josse, *Anal. Chem.* **79**, 1646 (2007).
- <sup>6</sup>P. A. Rasmussen, J. Thaysen, O. Hansen, S. C. Eriksen, and A. Boisen, *Ultramicroscopy* **97**, 371 (2003).
- <sup>7</sup>C. Ayela, T. Alava, D. Lagrange, D. Remiens, C. Soyer, T. Ondarcuhu, A. Greve, and L. Nicu, *IEEE Sens. J.* **8**, 210 (2008).
- <sup>8</sup>S. R. Manalis, S. C. Minne, and C. F. Quate, *Appl. Phys. Lett.* **68**, 871 (1996).
- <sup>9</sup>Y. S. Kim, H. J. Nam, S. M. Cho, J. W. Hong, D. C. Kim, and J. U. Bu, *Sens. Actuators, A* **103**, 122 (2003).
- <sup>10</sup>C. Ziegler, *Anal. Bioanal. Chem.* **379**, 946 (2004).
- <sup>11</sup>J. H. Seo and O. Brand, *J. Microelectromech. Syst.* **17**, 483 (2008).
- <sup>12</sup>L. Nicu and C. Bergaud, *J. Micromech. Microeng.* **14**, 727 (2004).
- <sup>13</sup>W. C. Xu, S. Choi, and J. Chae, *Appl. Phys. Lett.* **96**, 053703 (2010).
- <sup>14</sup>H. Zhang, W. Pang, M. S. Marma, C. Y. Lee, S. Kamal-Bahl, E. S. Kim, and C. E. McKenna, *Appl. Phys. Lett.* **96**, 123702 (2010).
- <sup>15</sup>L. Nicu, M. Guirardel, F. Chambosse, P. Rourgerie, S. Sinh, E. Trevisiol, J. M. Francois, J. P. Majoral, A. M. Caminade, E. Cattani, and C. Bergaud, *Sens. Actuators B* **110**, 125 (2005).
- <sup>16</sup>T. Xu, Z. H. Wang, and J. M. Miao, *Int. J. Nanotechnol.* **6**, 762 (2009).
- <sup>17</sup>T. Xu, Z. H. Wang, J. M. Miao, L. Yu, and C. M. Li, *Biosens. Bioelectron.* **24**, 638 (2008).
- <sup>18</sup>C. Ayela, F. Vandeveldel, D. Lagrange, K. Haupt, and L. Nicu, *Angew. Chem., Int. Ed.* **46**, 9271 (2007).
- <sup>19</sup>C. Ayela and L. Nicu, *Sens. Actuators B* **123**, 860 (2007).
- <sup>20</sup>M. Amabili and M. K. Kwak, *J. Fluids Struct.* **10**, 743 (1996).
- <sup>21</sup>T. Alava, N. Berthet-Duroire, C. Ayela, E. Trevisiol, M. Pugniere, Y. Morel, P. Rameil, and L. Nicu, *Sens. Actuators B* **138**, 532 (2009).
- <sup>22</sup>C. Ayela, L. Nicu, C. Soyer, E. Cattani, and C. Bergaud, *J. Appl. Phys.* **100**, 054908 (2006).
- <sup>23</sup>T. Alava, F. Mathieu, L. Mazenq, C. Soyer, D. Remiens, and L. Nicu, *J. Micromech. Microeng.* **20**, 075014 (2010).
- <sup>24</sup>See supplementary material at <http://dx.doi.org/10.1063/1.3486112> for frequency measurements.
- <sup>25</sup>H. Lamb, *Proc. R. Soc. London* **98**, 205 (1920).
- <sup>26</sup>T. Braun, V. Barwich, M. K. Ghatkesar, A. H. Bredekamp, C. Gerber, M. Hegner, and H. P. Lang, *Phys. Rev. E* **72**, 031907 (2005).